*Journal of Experimental Botany*
doi:10.1093/jxb/erx250

RESEARCH PAPER

# Crop-model assisted phenomics and genome-wide association study for climate adaptation of *indica* rice. 2. Thermal stress and spikelet sterility

**Michael Dingkuhn[1,*], Richard Pasco[2], Julie Mae Pasuquin[2], Jean Damo[2], Jean-Christophe Soulié[1], Louis-Marie Raboin[1], Julie Dusserre[1], Abdoulaye Sow[3], Baboucarr Manneh[3], Suchit Shrestha[2] and Tobias Kretzschmar[2]**

[1] Cirad, Umr AGAP (Dept BIOS) and Upr AIDA (Dept ES), F-34398, Montpellier, France
[2] IRRI, CESD Division, DAPO Box 7777, Metro Manila, Philippines
[3] Africa Rice Center, Sahel Station, PB 96, St Louis, Senegal

* Correspondence: m.dingkuhn@irri.org, dingkuhn@cirad.fr

Received 14 February 2017; Editorial decision 20 June 2017; Accepted 27 June 2017

Editor: Greg Rebetzke, CSIRO Agriculture and Food

## Abstract

**Low night and high day temperatures during sensitive reproductive stages cause spikelet sterility in rice. Phenotyping of tolerance traits in the field is difficult because of temporal interactions with phenology and organ temperature differing from ambient. Physiological models can be used to separate these effects. A 203-accession *indica* rice diversity panel was phenotyped for sterility in ten environments in Senegal and Madagascar and climate data were recorded. Here we report on sterility responses while a companion study reported on phenology. The objectives were to improve the RIDEV model of rice thermal sterility, to estimate response traits by fitting model parameters, and to link the response traits to genomic regions through genome-wide association studies (GWAS). RIDEV captured 64% of variation of sterility when cold acclimation during vegetative stage was simulated, but only 38% when it was not. The RIDEV parameters gave more and stronger quantitative trait loci (QTLs) than index variables derived more directly from observation. The 15 QTLs identified at $P<1 \times 10^{-5}$ (33 at $P<1 \times 10^{-4}$) were related to sterility effects of heat, cold, cold acclimation, or unexplained causes (baseline sterility). Nine annotated genes were found on average within the 50% linkage disequilibrium (LD) region. Among them, one to five plausible candidate genes per QTL were identified based on known expression profiles (organ, stage, stress factors) and function. Meiosis-, development- and flowering-related genes were frequent, as well a stress signaling kinases and transcription factors. Putative epigenetic factors such as DNA methylases or histone-related genes were frequent in cold-acclimation QTLs, and positive-effect alleles were frequent in cold-tolerant highland rice from Madagascar. The results indicate that epigenetic control of acclimation may be important in *indica* rice genotypes adapted to cool environments.**

**Key words:** Candidate genes, cold and heat tolerance, epigenetics, heuristics, male sterility, *Oryza sativa* L., RIDEV crop model.

## Introduction

Spikelet sterility of rice, in particular male sterility, has received scientific attention for three reasons: (i) yield losses due to sensitivity to abiotic stresses such as heat (Jagadish *et al.*, 2007), cold (Dingkuhn *et al.*, 1995; Dingkuhn, 1995), and drought (Sheoran and Sain, 1996); (ii) its importance in hybrid seed production (Wang *et al.*, 2013); and (iii) genetic

sterility barriers hampering intersubspecific (Long *et al.*, 2008) and interspecific (Garavito *et al.*, 2010) crosses in breeding. This study focused on thermal-stress-induced sterility and its genomic associations.

Heat and cold stress cause male sterility in different ways and at different stages of reproductive development. Cold stress disrupts cellular development processes at the microspore stage, notably meiosis (De Storme and Geelen, 2014). Pollen infertility may result from deregulation or sugar starvation of meiosis itself (Sheoran and Sain, 1996) or disturbed anther, tapetum, or pollen wall development (Wang *et al.*, 2013). Heat damage is rare at the microspore stage because the shoot apex is located near the bottom of the canopy under shaded conditions (Julia and Dingkuhn, 2013). The most heat-sensitive phase occurs at anthesis and can impair anther dehiscence, pollination, pollen germination or pollen tube growth (Jagadish *et al.*, 2007). Given the diversity of vulnerable processes, many genes and pathways are involved in sterility, depending on the causative stress and its phenological timing (De Storme and Geelen, 2014). Tolerance to heat also depends on constitutive pollen production, affecting probability of successful pollination under stress (Jagadish *et al.*, 2007). The female spikelet organs appear to be more resilient to thermal stresses (Wolters-Arts *et al.*, 2013) and the male parent chiefly determines the extent of heat-induced sterility (Fu *et al.*, 2015). Female organs, however, play a major role in the interspecific sterility barrier (Garavito *et al.*, 2010).

Unrelated to stress-induced sterility, empty spikelets may also occur under plant-scale assimilate shortage, spikelet-level assimilate import restrictions or unfavorable topological position of spikelets within the panicle (Yang and Zhang, 2010). Such positional effects may be enhanced by physiological stresses causing poor panicle exertion from the surrounding leaf sheaths, inducing spikelet sterility when peduncles stay short (O'Toole and Namuco, 1983; Julia and Dingkuhn, 2013). Consequently, thermal spikelet sterility can occur at pre-floral stages through impeded development of male organs or indirectly through inhibited peduncle elongation, or at anthesis when pollination occurs.

We study here the incidence of unfilled spikelets, summarily termed sterility, on 203 diverse *indica* rices (the *indica* subset of the ORYTAGE diversity panel; http://ricephenonetwork.irri.org/diversity-panels/orytage-diversity-panels) grown in ten climatically contrasting environments. A heuristic, model-based approach was used to disaggregate the observed sterility into causal components dependent on the environmental conditions they were associated with during critical phenological stages. Proof of concept for this approach was previously provided by Reymond *et al.* (2003) for drought, Rebolledo *et al.* (2015) for early vigor, and Yin *et al.* (2005) and Dingkuhn *et al.* (2017) for phenology, yielding quantitative trait loci (QTLs) that would not have been discovered with untransformed phenotype data.

The RIDEV model, first published by Dingkuhn *et al.* (1995) and Dingkuhn and Miezan (1995) (and under this name by Wopereis *et al.*, 2003), was used in revised form (V2) in the companion study (Dingkuhn *et al.*, 2017) for phenology traits. Here it was further improved to simulate thermal sterility estimated from microclimate-based organ temperatures (shoot apex at microspore stage and panicle at anthesis) by using rice microclimate *vs* sterility relationships published elsewhere (Julia and Dingkuhn, 2012, 2013). We also introduced an acclimation parameter implementing a hardening effect of stress exposure during earlier phenological stages. Such mechanisms were reported by Shimono *et al.* (2010).

This study aimed at (i) heuristically phenotyping the ORYTAGE *indica* rice diversity panel using RIDEV V2, thereby considering fitted crop parameter values as genotypic traits; (ii) conducting genome-wide association studies (GWAS) for RIDEV V2 parameters and, by comparison, for simpler phenotypic index variables previously reported (Dingkuhn *et al.*, 2015*a*); and (iii) identifying potential candidate genes.

## Materials and methods

Experiments and germplasm were described by Dingkuhn *et al.* (2015*a*,b) and the companion paper (Dingkuhn *et al.*, 2017). Genotyping and GWAS are described in the companion paper. Essential information is repeated here.

### *Experimental design*

#### *Experiment in Senegal*

The experiment was conducted at the AfricaRice Sahel Station at Ndiaye, Senegal (16°12′N, 16°16′W, 8 m above sea level; asl) with an augmented design with six blocks, two factors (six sowing dates, 203 genotypes) and four replicated checks (IR64, Sahel 108, N22, Chomrong). Subplots were 1 m×1 m and pre-germinated seed was sown at 20 cm×20 cm. Fields were flooded throughout. Fertilizer inputs were 120–60–60 (N–P–K, kg ha$^{-1}$). Sowing dates were 7 February 2009, 7 March 2009, 7 April 2009, 17 July 2009, 17 September 2009 and 19 October 2009.

Population-level spikelet sterility was measured on plants at the center of subplots. All panicles of eight hills were collected, counted, and spikelets stripped off, bulked, separated into filled and unfilled spikelets, oven-dried and weighed. Mean spikelet weight was determined from 200 filled and 200 unfilled spikelets. Flowering dates were recorded.

#### *Experiment in Madagascar*

Experimental sites were Ambohitromby (Hautes Terres, Région d'Antsirabe, 19°52′S, 46°59′E, 1494 m asl) and Ivory (19°32′S, 46°24′E, 869 m asl). The experiment, identical at both sites, was a randomized complete block design with three replications. Elemental plots (variety) were 0.6 m×1.4 m (3 × 7 hills planted at 20 cm×20 cm, with the central row used for observations). Check varieties were as in Senegal but cv. Chomrong was absent.

Pre-germinated seed was sown on 3 December 2009 and 6 December 2010 at Ivory and on 11 December 2009 and 15 December 2010 at Ambohitromby in a seedling nursery and transplanted as single plants 15–20 d after sowing. Plots were kept flooded at 5–10 cm. Fertilizer was applied as green manure (5 t ha$^{-1}$), 81 kg ha$^{-1}$ N as urea, 27 kg ha$^{-1}$ P as triple superphosphate and 49 kg ha$^{-1}$ K as KCl. Spikelet sterility was measured as described for Senegal but on the five central plants on the middle row of the plots.

### *Germplasm*

The population was taken from the ORYTAGE species-wide (*O. sativa* L.) diversity panel of Cirad (http://ricephenonetwork.irri.org/diversity-panels/orytage-diversity-panels) which is also a resource for the GRiSP Global Rice Phenotyping Network (http://ricephenonetwork.irri.org). A subsample of 203 *indica* accessions was grown (see Supplementary Table S1 at *JXB* online).

*Genomics data resource and association mapping*

Genotyping was conducted at Diversity Arrays Technology Pty Ltd. (Australia) using genotyping by sequencing (GBS) as described by Courtois *et al.* (2013) and Dingkuhn *et al.* (2017). Data cleaning involved removing sequences having more than one hit on the pseudomolecules, which were discarded, as well as markers with call rates ≤80% or minor allele frequency ≤2.5%. After data cleaning and before imputation of the GBS resource, the rate of missing data was 6.5%. The final data set had 16 232 markers (8214 DArT and 8018 single nucleotide polymorphism (SNP) markers), giving an average density of one marker per 24 kb. There were nine gaps of more than 500 kb devoid of markers on chromosomes 2, 4, 6, 7, 8, and 11, of which two were of approximately 1 Mb.

GWAS was conducted for each trait using a mixed model with control of the structure and kinship under Tassel v5.0 (Bradbury *et al.*, 2007). Kinship was computed using Tassel v5. The genetic structure of the panel is presented in Supplementary Fig. S1. The threshold to declare an association highly significant was set at $P<1 \times 10^{-5}$. Associations having $1 \times 10^{-5}<P<1 \times 10^{-4}$ are presented in Supplementary Table S2. The 50% decay genomic distance of linkage (LD) was calculated according to Sved (1971). Supporting SNPs were defined as SNPs with $P<1 \times 10^{-3}$ located within ±LD. Quantile–quantile plots for the GWAS are presented in Supplementary Fig. S2.

*RIDEV V2 model*

The model is described in detail in the companion paper (Dingkuhn *et al.*, 2017) and only essential information is provided, namely on spikelet sterility simulations.

*General*

The RIDEV V2 model is an improved version of RIDEV described and validated by Dingkuhn *et al.* (1995), Dingkuhn and Miezan (1995) and Dingkuhn (1995), and later described as an agronomic decision tool by Wopereis *et al.* (2003). It simulates the duration of phenological phases, the timing of panicle initiation (PI) and flowering (FL) events, and the incidence of cold- or heat-induced sterility. The model can be used in simulation mode (phenology/sterility prediction) or heuristic (reverse) mode to estimate genotypic parameters. Table 1 presents the variables and parameters used in this study.

*Spikelet sterility*

Similar to the original RIDEV (Dingkuhn, 1995), RIDEV V2 simulates three sources of sterility: (i) an unexplained baseline level set by parameter *KSterBase*, (ii) chilling set by *KSterCold* and *KSterSlope*, and (iii) heat set by *KSterHeat*. Baseline sterility is a constant spikelet fraction. Cold sterility is driven by the mean minimum water temperature ($T_{w(min)}$) during the microspore stage (about the booting stage), estimated to occur between 0.3 and 0.8 of the RPR stage (equal to 120–320 °C d before flowering in this study, or about 9–23 d in a warm environment). Heat sterility is driven by the panicle temperature ($T_{pan}$) during the time of day of anthesis and averaged for the period −60 to+60 °C d around flowering, a period of *ca*. 9 d. The timing of these phases is determined by the phenology modules described in the companion paper. The phenological windows were chosen wide to account for uncertainty.

Two examples of observed sterility response to low $T_{w(min)}$ are given in Fig. 1B. Figure 1C describes the broken-stick linear models implemented to simulate the three different components of sterility, and the equation that provides total sterility. For data supporting the phenological and factor hypotheses for thermal sterility, refer to Dingkuhn *et al.* (1995). The C++ source code of the present version of RIDEV is given in Supplementary Protocol S1.

*Development*

RIDEV simulates crop development from sowing until physiological maturity, whereby crop establishment is included in the basic vegetative phase (BVP). The BVP is followed by a photoperiod-sensitive phase (PSP) ending at PI, a reproductive phase (RPR) ending at FL and a maturation phase (MATU). Each of these phases except PSP has a genotypic thermal-time budget. Duration of PSP depends on photoperiod and thermal time using the *Impatience* model (Dingkuhn *et al.*, 2008). Thermal time calculation uses genotypic cardinal temperatures *Tbase* and *Topt* (Dingkuhn and Miezan, 1995) and a standard diurnal temperature pattern. Depending on

**Table 1.** *RIDEV V2 parameters and input/output variables used in this study*

*X* ... *Y* denotes biologically reasonable ranges.

| Parameter/variable | Definition |
|---|---|
| Scenario parameters | |
| *Latitude* | xx.yy, decimal (degrees) |
| *SowingDate* | dd/mm/yyyy |
| *Transplanting* | 0 or 1, binary |
| *DDTransplantingShock* | 0 ... 200 (default=100), development lag in thermal time units (°C d) |
| *POP* | Plant population density, 50 000 ... 1 000 000 (plants $ha^{-1}$) |
| Input variables (variables in brackets only needed for heat sterility under flooded cultivation) | |
| *Tmin* | Daily minimum air temperature at 2 m (°C) |
| *Tmax* | Daily maximum air temperature at 2 m (°C) |
| Crop parameters for phenology (can be optimized by R-Genoud) | |
| *KSterBase* | Baseline sterility that cannot be explained by thermal stresses, 0 ... 1 (typically 0.1 to 0.2) (fraction) |
| *KSterCold* | Critical $T_{min(apex)}$ at microspore stage for onset of cold stress, 20 ... 0 (°C) |
| *KSterSlope* | Sensitivity of chilling response: *T* interval (°C) for sterility to rise from zero to 100% |
| *KSterHeat* | Critical $T_{pan}$ for onset of heat stress, at TOA during the flowering period, 25 ... 40 (°C) |
| *AcclimSterC* | Acclimation effect of low $T_{min}$ during BVP (<18 °C), reducing *KSterCold* (effective at microspore stage), 0 ... 15 |
| Output variables | |
| *SterBase* | Baseline (non-stress related) sterility (%) |
| *SterCold* | Cold sterility (%) |
| *SterHeat* | Heat sterility (%) |
| *SterTot* | Total sterility (non-additive) (%) |

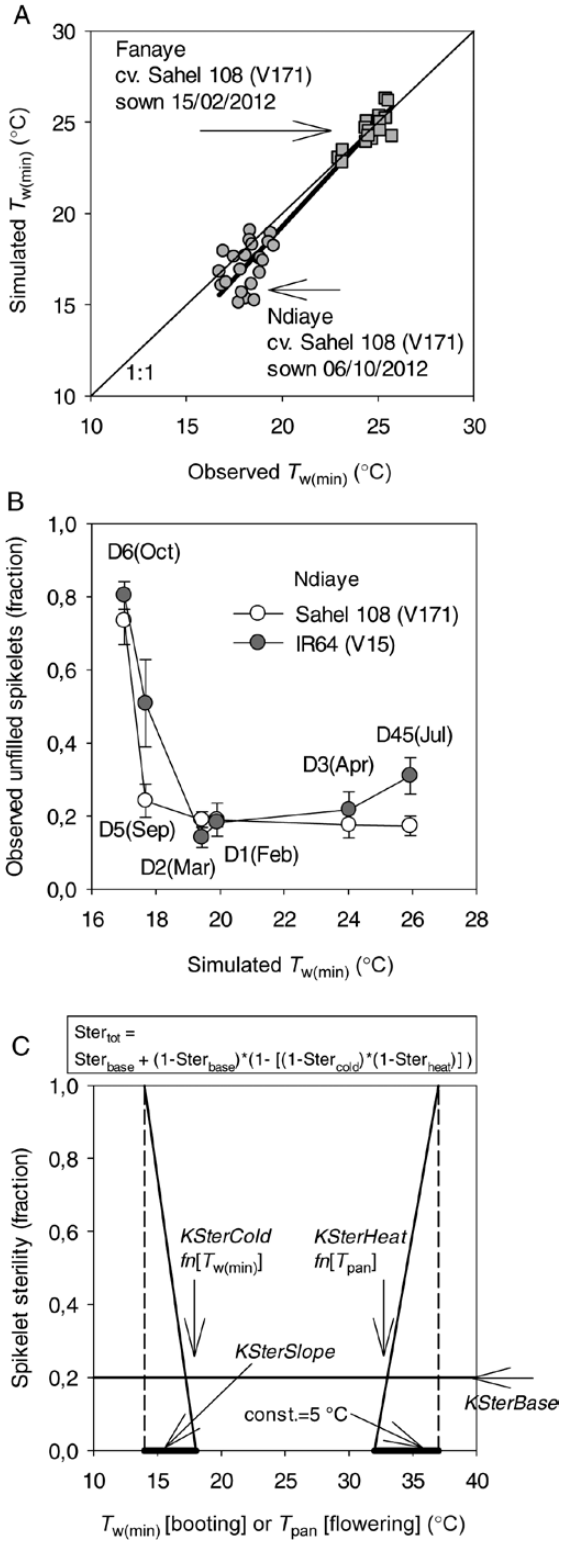


**Fig. 1.** (A) Validation of RIDEV simulation of daily minimum water temperature ($T_{w(min)}$) during the 21 d preceding maximum flowering, using independent data measured at Ndiaye (cold-dry season) and at Fanaye, a site located *ca*. 130 km east of Ndiaye. (B) Relationship between observed fraction of unfilled spikelets (mean±SE) and simulated $T_{w(min)}$ at booting stage for two replicated check cultivars for the six sowing dates in Senegal in the phenotyping experiment. (C) Schematic diagram and equation to for calculation of total spikelet sterility and its components. $Ster_{tot}$, total sterility; $Ster_{base}$, baseline sterility; $Ster_{cold}$, cold stress induced sterility; $Ster_{heat}$, heat stress induced sterility. The RIDEV crop parameters *KSterCold*, *KSterSlope*, *KSterHeat* and *KSterBase* are defined in Table 1.

location in the canopy of the shoot apex, temperatures of air or floodwater are used.

*Water and apex temperature*

The shoot apex of irrigated rice is submerged until booting (stem elongation) stage. Daily minimum and maximum water temperature ($T_w$) are simulated from leaf area index as described in the companion paper (Dingkuhn *et al.*, 2017). Apex temperature ($T_{apex}$) is equal to $T_w$ while the apex is under the water line. Internode elongation lifts the apex nearly to the canopy top and the apex assumes air temperature.

*Panicle temperature*

Data from an extensive study by Julia and Dingkuhn (2013), describing the rice Panicle temperature ($T_{pan}$) relationship with microclimate in multiple field environments in Senegal and the Philippines by infrared imagery, were revisited to generate an empirical model predicting $T_{pan}$. Multiple, stepwise, linear regression of 2941 infrared-based temperature difference measurements ($T_D$=$T_{a(2m)}$−$T_{pan}$) observations *vs* simultaneous crop and weather observations at 2 m resulted in the following model:

$$T_D = 0.782 + 0.422T_a - 0.0443\mathrm{RH} - 0.00287R_s - 8.05Z - 6.59\mathrm{LTR} \quad (1)$$

where $T_D$ (°C) is the temperature difference between air (at 2 m) and panicle temperature; $T_{a(2m)}$ (°C) is air temperature at 2 m; RH (%) is air relative humidity; $R_s$ (W m$^{-2}$) is solar radiation; $Z$ (m m$^{-1}$) is the ratio of ground height of the center of the panicle to plant height; and LTR is light transmission ratio of the canopy as calculated from LAI using the Lambert–Beer law and $K_{ext}$=0.5. This model had an adjusted $R^2$ of 0.82, standardized coefficients of 0.63 ($T_a$), −0.30 (RH), −0.14 ($R_s$), −0.19 ($Z$), and −0.13 (LTR). The *F*-value was 2613. Figure 2 shows for check cultivars the calculated *vs* observed TD for Senegal (November and February sowings).

*Time of day of anthesis*

Prediction of time of day of anthesis (TOA) is needed to compute $T_{pan}$ at anthesis, which happens during 2 h usually in the morning, but depends on the weather. RIDEV uses finding of Julia and Dingkuhn (2012) that mean $T_{min(air)}$ during the 7 d preceding anthesis is predictive of TOA (with mean TOA=14−0.4 $T_{min}$), TOA being expressed as hours after sunrise. This approximation described well the variation of TOA for four check varieties, which were similar. We generalized this relationship for the diversity panel. Panicle temperature at TOA was calculated by hourly interpolation. For this, RIDEV generates hourly estimations of temperature from daily $T_{min}$ and $T_{max}$, day length and an empirical diurnal pattern (see Supplementary Fig. S3).

*Acclimation of sterility response to cold conditions*

Parameter estimation mostly provided accurate phenotype simulations across the ten environments, but for some genotypes this was not the case. We hypothesized that this was caused by cold acclimation at high altitude in Madagascar whereas in Senegal, periods with cold nights were short and seasonal (Dingkuhn *et al.*, 2015*b*). An optional function was implemented that reduces *KSterCold* (temperature below which cold-induced sterility occurs) when the crop experienced cold at the vegetative stage, using the genotypic coefficient *AcclimSterC*. The decrease of *KCritSter* following acclimation is the product of *AcclimSterC* and the number of degrees Celsius by which mean $T_{min(air)}$ is below 18 °C during the basic vegetative phase (BVP). Dingkuhn *et al.* (1995) reported 18 °C to be the critical $T_{w(min)}$ below which cold-induced sterility occurs in many rice cultivars.

The equation calculating cold sterility is as follows, with the additional component of cold acclimation shown in bold:

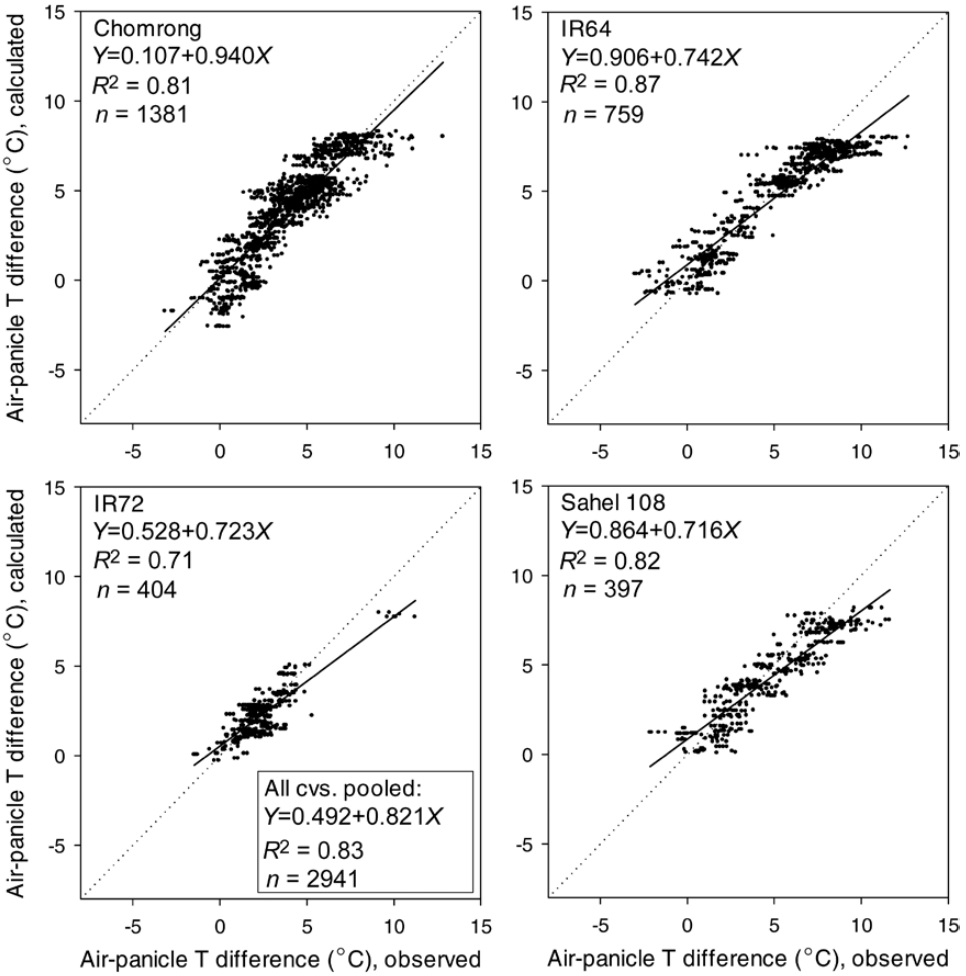


**Fig. 2.** Correlation between calculated and observed air–panicle temperature difference across different seasons and times of day in Senegal using RIDEV model equation, for four check cultivars. Data from Julia and Dingkuhn (2013) re-analysed.

$$\text{Cold sterility}(\text{fraction spikelets}) = \min(1, \max\ (0, (KSterCold - (\boldsymbol{AcclimSterC} \times \mathbf{max}\ (\mathbf{0},\ \mathbf{18} - T_{w(min)}[\mathbf{mean},\ \mathbf{BVP}])) - T_{w(min)}[\mathbf{mean},\ \mathbf{booting\ stage}]) / KSterSlope)) \quad (2)$$

*AcclimSterC* thus reduces the cold sensitivity (*KCritSter*) of sterility during the microspore stage in cases where the crop experienced cold conditions during BVP.

### *RIDEV variables and parameters*

Table 1 presents an overview of RIDEV V2 variables and parameters used in the sterility study. A complete list is presented in Supplementary Table S3. As weather input, daily air $T_{min}$ and $T_{max}$ (°C), solar radiation $R_s$ (MJ), and minimum and maximum relative humidity HR (%) were used. The following crop parameters were used to simulate *Tapex* (cold stress at microspore stage) and *Tpan* (heat stress at anthesis) which determine sterility:

*Z*: the relative position *Z* of the panicle relative to plant tops (ground height), set to default=0.8
*POP*: plant population density (plants $ha^{-1}$), whose value depended on the experiment
*PLAini*: initial leaf area per plant, set to default=0.0001 ($m^2$)
*LRGRmax*: leaf area relative growth rate, set to 1.3 (unitless)
*LAImax*: maximal leaf area index, set to 5 (unitless)

(The last four parameters were needed to implement a standard LAI time course that served to estimate LTR, affecting microclimate.)

Genotypic parameters for crop phenology were estimated by optimization procedures as described in the companion paper (Dingkuhn *et al.*, 2017; Run3 which simulated phenotype best). The genotypic parameters for sterility, the object of the present study, were estimated the same way with phenology parameters fixed to values estimated previously.

### *Parameters and ranges for estimation of genotypic values*

The genotypic parameters estimated by optimization, thereafter considered as genotypic traits, were as follows:

*KSterBase*: unexplained sterility (fraction), estimation boundaries 0…1
*KSterCold*: critical $T_{min(apex)}$ for cold sterility (°C), estimation boundaries 20 ... 5
*KSterHeat*: critical $T_{pan}$ at TOA for heat sterility (°C), estimation boundaries 20 ... 40
*KSterSlope*: temperature interval below *KSterCold* causing 100% sterility (°C). No slope parameter was used for the heat response of sterility and the model used a fixed coefficient of 5 (sterility attains 100% if *Tpan* at TOA attains the value of *KSterHeat*+5 °C). Estimation boundaries 2 ... 15
*AcclimSterC*: acclimation response of *KSterCold* to chilling during BVP, estimation boundaries 0 ... 15

Parameters were either fixed to default values or optimized by R-Genoud (Dingkuhn *et al.*, 2017) within physiologically relevant boundaries, with all parameters optimized in one procedure. The

accuracy of predicted *vs* observed sterility across environments was evaluated by normalized-least square error method (cost function). R-Genoud varied parameter values to minimize the cost function. Table 2 presents the four combinations of optimized parameters used in this study (estimation runs), namely Run1 and Run2 without considering acclimation and Run3 and Run4 with it. In Run2 and Run4, *KSterSlope* was fixed to the default value to reduce parameter number. (A smaller number sometimes improved GWAS associations but reduced accuracy of phenotype prediction.)

### *Traits analysed by GWAS*

Two types of traits were analysed: (i) index variables directly calculated from measurements and (ii) estimated RIDEV parameters. The index variables were described in detail by Dingkuhn *et al.* (2015*a*) and are summarized as follows:

Ster_20C *(fraction spikelets)*
Estimates sterility incidence at Tw(min)=20 °C, based on the observed correlations of sterility *vs* Tw(min) at microspore stage across all environments.

Ster_Slope *(°C–1)*
Correlations were used to estimate the rate of increase of sterility for $T_{w(min)}$ below 18 °C. Frequency distributions are presented in Supplementary Fig. S4. The other traits used for GWAS were the RIDEV parameters listed in Table 2, *KSterBase*, *KSterCold*, *KSterHeat*, *KSterSlope*, and *AcclimSterC*.

### *Searches for annotated genes associated with the QTLs detected*

Annotated genes within ±100 kB of a peak SNP were extracted from Phytozome (Joint Genome Institute JGI), https://phytozome.jgi.doe.gov) and MSU database (Michigan SU, http://rice.plantbiology.msu.edu/). Functional and expression-related information was extracted from GeneVisible (https://genevisible.com/), PlaNet (http://aranet.mpimp-golm.mpg.de/), Gramene (http://archive.gramene.org/), UniProt (http://www.uniprot.org/), RiceXPro (http://ricexpro.dna.affrc.go.jp/), RiceChip (http://www.ricechip.org/) and gabi (https://www.gabipd.org/). Genes within ±39 kB (estimated LD; Dingkuhn *et al.*, 2017) were considered as likely candidates if supported by function.

### *Statistics*

Linear regression analyses and frequency distributions were conducted with SigmaPlot 12.3 (Systat Sofwares Inc.).

## Results

### *Sensitivity analysis for crop parameters*

The effect of crop parameter variation on sterility simulations was evaluated for the four most contrasting environments (see Supplementary Fig. S5). Each environment caused different patterns of parameter effects. Consequently, there was sufficient environmental diversity in this study to disaggregate component traits of sterility (parameters optimized). The only similarity in environment response was for *KSterCold* (critical *T*) *vs KSterSlope* (1/slope) for the cold response, and we thus conducted estimation runs for either both parameters or only *KSterCold* (Table 2).

### *Estimated RIDEV parameters*

Estimated RIDEV parameter value distributions are presented in Fig. 3. The histograms describe the entire panel as previously characterized for phenology (Dingkuhn *et al.*, 2015*b*) and sterility phenomics (Dingkuhn *et al.*, 2015*a*) with 203 accessions. *KSterBase* was not included because its effect is environment independent.

*KSterBase* (unexplained baseline sterility) had a normal distribution centered at 0.10–0.15 but showed an upward tail constituted by only a few accessions, with a maximal value of 0.5 (Fig. 3A). The vast majority of accessions had baseline sterility below 0.2 (20% of spikelets). For *KSterSlope* ($T_{min}$ interval within which sterility increases from zero to 100%) (Fig. 3B), a value of <2.5 °C was observed for about half of the accessions, indicating a steep response of sterility to temperature. The other accessions showed a broad distribution of higher *KSterSlope* values up to 10.5 °C. The critical temperature *KSterCold* (Fig. 3C) showed normal distribution centered at about 18 °C, with only few accessions outside the 17–20 °C range. For the *KSterHeat* critical temperature (Fig. 3D), the vast majority of accessions ranged between 29 and 33 °C but some had higher values. Since extreme heat occurred rarely, *KCritHeat* estimations above 35 °C are uncertain and mean that heat-induced sterility was absent.

Cold-acclimation parameter *AcclimSterC* was estimated with either the *KSterSlope* co-optimized (Run3, Fig. 3E) or set to the value 5 (Run4, Fig. 3F). Most accessions (70% for Run3) had estimated values ≤1, 20% were between 1 and 2, and only 10% had greater values between 2 and 12. Fixing the value of *KSterSlope* had little effect on this distribution (Run4), but both estimations of *AcclimSterC* were retained because the GWAS results were different. The parameter distributions indicate that most accessions showed little acclimation, but a small subset showed strong acclimation.

**Table 2.** *RIDEV parameter estimation runs*

Fields marked × indicate inclusion in estimation run.

| Parameter estimation run | Environments | | Crop parameters estimated | | | | | Figures |
|---|---|---|---|---|---|---|---|---|
| | Senegal | Madagascar | *KSterBase* | *KSterCold* | *KSterSlope* | *KSterHeat* | *AcclimSterC* | |
| 1 | 6 | 4 | × | × | × | × | Set to 0 | 3B, 4B, C, D |
| 2 | 6 | 4 | × | × | Set to 5 | × | Set to 0 | 3C |
| 3 | 6 | 4 | × | × | × | × | × | 6A |
| 4 | 6 | 4 | × | × | Set to 5 | × | × | 6B |

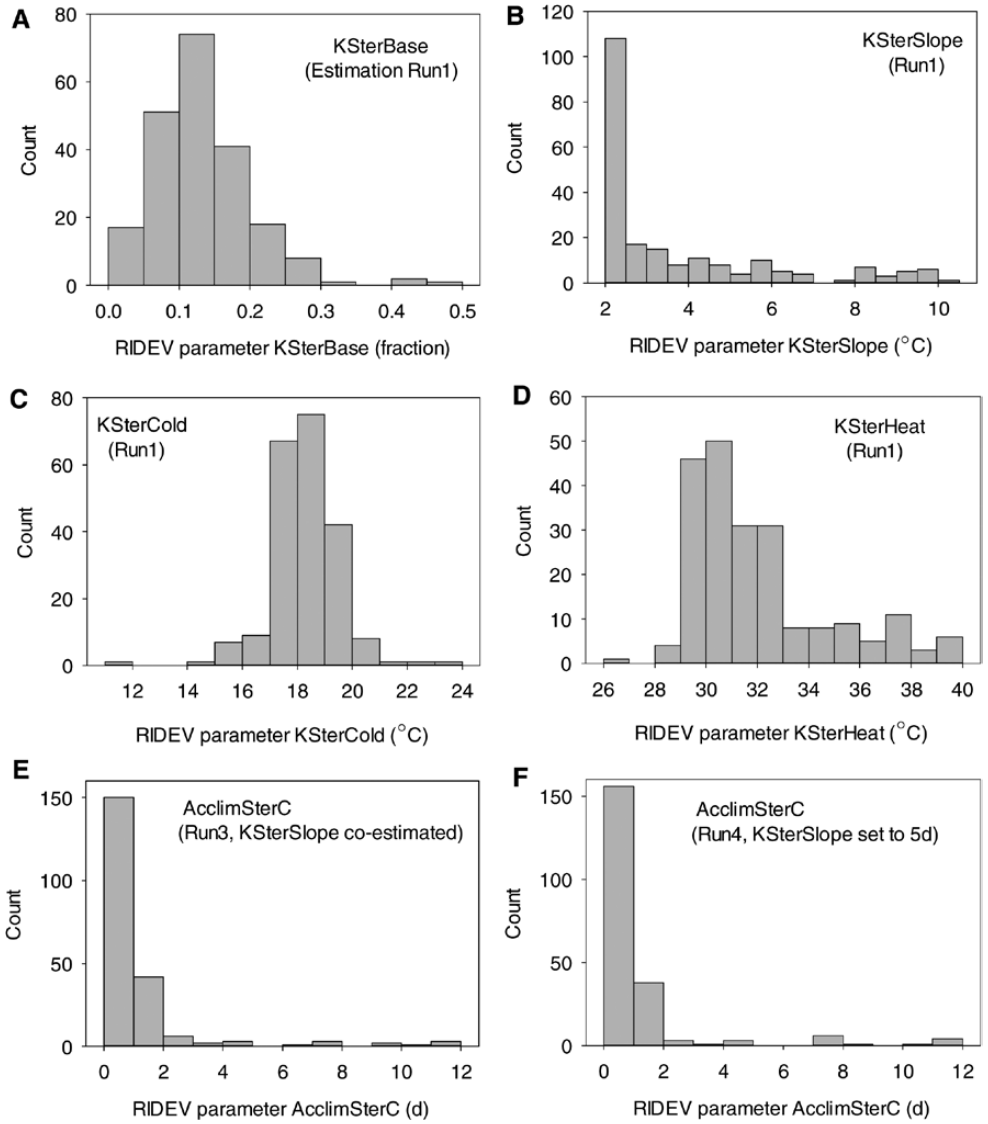


**Fig. 3.** Frequency distributions of RIDEV parameter values for spikelet sterility for the ORYTAGE *indica* panel.

### *Variation in spikelet sterility explained by RIDEV*

The RIDEV model explained about two-thirds of observed variation in sterility across all accessions and environments (Run3 and Run4). Regression analyses of simulated ($Y$) *vs* observed sterility ($X$), sterility expressed as a fraction, gave the following. Senegal subset: $Y$=0.045 + 0.717$X$, $R^2$=0.70****, $n$=1098; Madagascar subset: $Y$=0.037 + 0.622$X$, $R^2$=0.61****, $n$=865. All environments: $Y$=0.043 + 0.652X, $R^2$=0.64****, $n$=1963. For check variety Sahel 108 alone, the correlation was as follows: All environments: $Y$=0.019 + 0.738$X$, $R^2$=0.77***, $n$=48.

The one-third unexplained sterility (or one-fourth for the check) was probably caused by the high intrinsic biological variation of sterility incidence, which responds to many factors, and error propagation from phenology to sterility simulations, causing errors in the timing of sensitive phenological phases.

Several alternative hypotheses to acclimation were tested but did not further improve predictions. When setting *AcclimSterC*=0 (disabling acclimation), RIDEV explained only 38% of observed sterility: $Y$=0.083 + 0.456$X$, $R^2$=0.38***, $n$=1963.

Consequently, the phenomenon captured with *AcclimSter* impacted strongly on spikelet sterility.

### *Genomic associations for baseline sterility*

Associations for unexplained baseline sterility are presented in Fig. 4 (details in Table 3). Two major QTLs ($P<1.0 \times 10^{-5}$) were observed for index variable *Ster_20C*, *Sb2(1)i* (chr2) and *Sb11i* (chr11). A minor QTL having $P=4.0 \times 10^{-5}$ (*Sb6(1)i*) supported by nine SNPs was located on chr6. *KSterBase*, conveying similar information as *Ster_20C*, yielded two major QTLs on chr6 (*Sb6(2)m*) and chr8 (*Sb8m*). None colocalized with QTLs for *Ster_20C*. However, there were similarities in the Manhattan plots (Fig. 4A *vs* 4B). Minor QTLs on chr4, 6 and 8 colocalized in both diagrams, and major RIDEV QTL *Sb8m* (Fig. 4B) was also discernible in Fig. 3A. Associations changed slightly when the model parameter *KSterSlope* was fixed to a constant value to avoid overparameterization (Fig. 4C). While most peaks diminished, QTL *Sb6(2)m* strongly increased to attain $P=4.0 \times 10^{-8}$.

*Genomic associations for sterility response to temperature*

The correlation-derived index variable *Ster_Slope* gave three QTLs on chr2, 3 and 7 (Fig. 5A). Major QTL *Ss2i* was supported by 22 SNPs and had high allele frequency (21%) whereas *Ss3i* and *Ss7i* were isolated SNPs with low allelic frequency (see Supplementary Table S2). Minor QTL *Ss1i* on chr1 was supported by 13 SNPs ($P$=2.5 × $10^{-5}$).

No major QTL was detected for parameter *KSterCold* (Fig. 5B; *Sc10m* was classified as minor due to absence of supporting SNPs) and one was found for *KSterHeat* (Fig. 5D: *Sh4m*). No significant association was observed for *KSterSlope* (Fig. 5C). However, when *KSterSlope* was fixed to constant value (Run2), *KSterCold* which then absorbed the variation of both slope and critical temperature gave three highly significant associations (Fig. 6), *Sc1m* and *Sc6m*

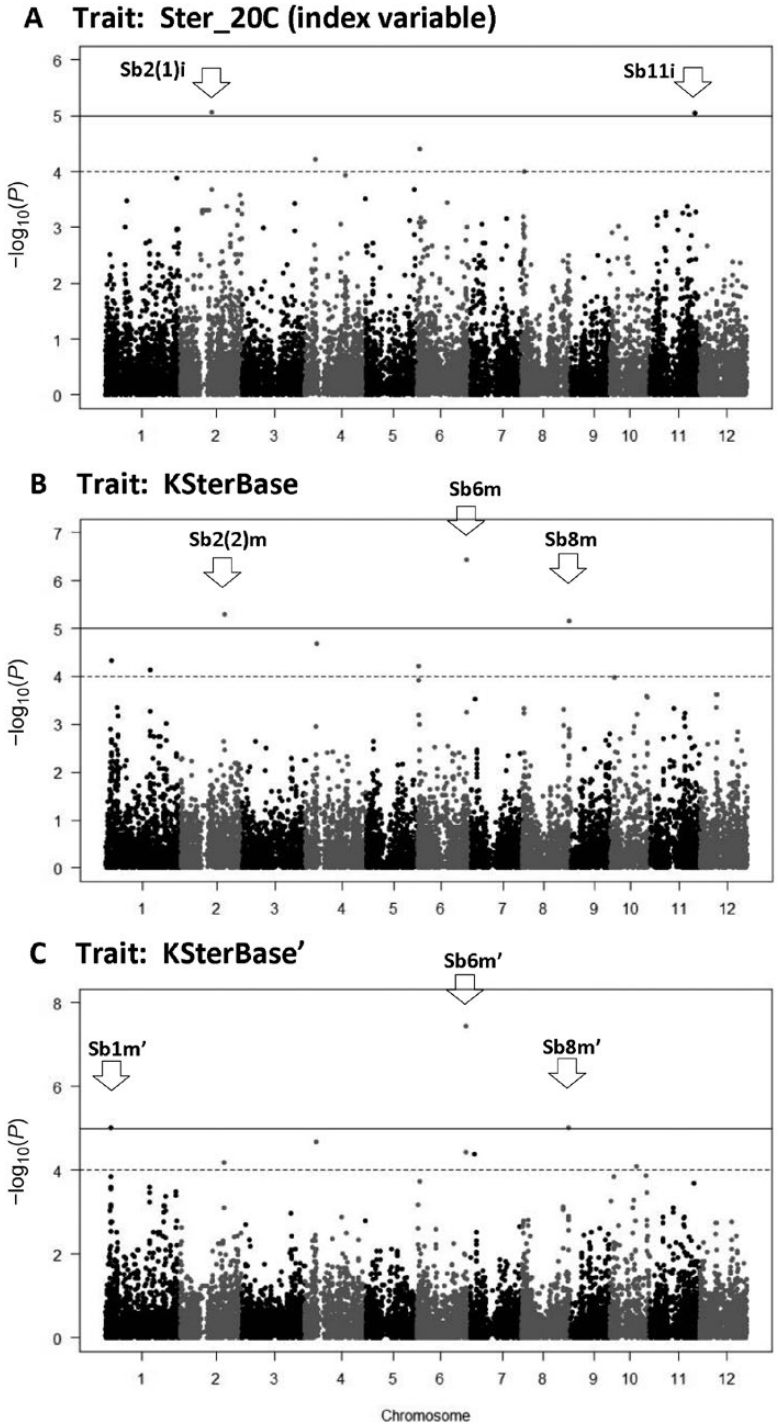


**Fig. 4.** GWAS associations for baseline sterility in the absence of thermal stress. (A) Index variable *Ster_20C* derived from regression analysis. (B) RIDEV parameter *KSterBase* estimated with co-fitting of RIDEV slope parameter (Estimation Run1, Table 2). (C) *KSterBase* estimated with parameter *KSterSlope* fixed to constant value (Run2).

**Table 3.** *GWAS associations and putative candidate genes for major QTLs (for complete list including minor QTLs refer to Supplementary Table S2)*

QTLs are identified by name, trait (for RIDEV estimation runs see Table 2), variable type and figure showing the Manhattan plot. Physical parameters for QTLs are chromosome number, locus and *P* for most significant SNP, number of supporting SNPs *P*<0.001 within LD, QTL effect on phenotype, base pair of main SNP, allele frequency (number accessions), and number of annotated genes within ±100 kB. Genes are shown in bold when located within LD (±39 kb). Distance of gene center from main SNP (kb) is provided in brackets. Gene function is provided as available from public databases.

| QTL | Trait, model run | Variable type | Chr | Locus of smallest *P* (bp) | P | SNPs *P*<0.001 | Effect | Base pair | | Allele frequency (no. of cases) | | No. genes | Fig | Putative candidate genes: LOC_ annotation(MSU), (distance from SNP in kB), (common name and function using public databases) |
|---|---|---|---|---|---|---|---|---|---|---|---|---|---|---|
| QTLs for sterility not related to thermal stress | | | | | | | | | | | | | | |
| *Sb2(1)i* | *Ster_20C* | Index | 2 | 18620629 | 7.9E–06 | 22 | 0.100 | G | A | 161 | 29 | 18 | 4A | **Loc_Os02g31140 [20]**, curly leaf, cuticle development |
| *Sb11i* | *Ster_20C* | Index | 11 | 26684031 | 1.0E–05 | 9 | –0.141 | T | A | 15 | 175 | 23 | 4A | **Loc_Os11g44170 [0]**, calmodulin-binding prot.; Loc_Os11g44250 [59]/Loc_Os11g44260 [68], serine/threonine kinase |
| *Sb8m* | *KSterBase* Run1 | Model | 8 | 27353014 | 7.9E–06 | 7 | –0.135 | C | A | 183 | 6 | 26 | 4B | Loc_Os08g43160 [56], serine/threonine kinase, TCP-TF; Loc_Os08g43190 [36], alcohol dehydrogenase; **Loc_Os08g43200 [32]**, dehydration/drought TF; **Loc_Os08g43270 [5]**, anti-apoptotic BCL2 enhancing, protection from ROS; **Loc_Os08g43334 [33]**, heat shock prot., drought+salt tol.; Loc_Os08g43380 [58], RAB GTPase, cold response |
| *Sb6(2)m′* | *KSterBase′* Run2 | Model | 6 | 28957091 | 4.0E–08 | 4 | –0.241 | A | G | 183 | 6 | 29 | 4C | Loc_Os06g47740 [67]/Loc_Os06g47750 [57]/**Loc_Os06g47820 [15]**, serine/threonine kinase; **Loc_Os06g47800 [29]**, apoptotic prot.; **Loc_Os06g47880 [11]**, cell division control, protein kinase; Loc_Os06g48000 [66]/Loc_Os06g48010 [71], peroxidases |
| *Sb8m′* | *KSterBase′* Run2 | Model | 8 | 27353014 | 1.0E–05 | 6 | –0.137 | C | A | 183 | 6 | 26 | 4C | As in *Sb8m* |
| QTLs for sterility related to thermal stress | | | | | | | | | | | | | | |
| *Ss2i* | *Ster_slope* | Index | 2 | 22320801 | 7.9E–06 | 22 | 0.042 | A | T | 153 | 37 | 16 | 5A | Loc_Os02g36880 [61], NAM no apical meristem protein; Loc_Os02g36890 [52], MYB-like TF, **Loc_Os02g36924 [23]**, syn. *OsMADS27*, seed development, up-regulated under osmotic stress, **Loc_Os02g36974 [16]**, chaperone; **Loc_Os02g36990 [21]**, dynein/microtubule |
| *Sh4m* | *KSterHeat* Run1 | Model | 4 | 29495307 29497328 | 2.0E–06 | 16 | –4.46 | T | G | 180 | 9 | 27 | 5D | **Loc_Os04g49410 [8]**, pollen prot., allergen; **Loc_Os04g49510 [37]**, serine/threonine kinase; **Loc_Os04g49420 [7]**, histone H4; **Loc_Os04g49430 [1]**, Zn-finger TF for root/shoot growth; **Loc_Os04g49450 [7]**, MYB-like TF; Loc_Os04g49530 [45], RAS family |

**Table 3.** *Continued*

| QTL | Trait, model run | Variable type | Chr | Locus of smallest *P* (bp) | P | SNPs *P*<0.001 | Effect | Base pair | | Allele frequency (no. of cases) | | No. genes | Fig | Putative candidate genes: LOC_ annotation(MSU), (distance from SNP in kB), (common name and function using public databases) |
|---|---|---|---|---|---|---|---|---|---|---|---|---|---|---|
| *Sc7m* | *KSterCold* Run2 | Model | 7 | 23251129 | 4.0E–07 | 9 | 6.14 | G | C | 184 | 6 | 40 | 6 | **Loc_Os07g38730 [6]**, GTPase with tubulin domain, flower devl., flag leaf senescence; **Loc_Os07g38760 [10]**, HEAT repeat prot.; Loc_Os07g38850 [55], prenyl transferase |
| Acclimation related QTLs | | | | | | | | | | | | | | |
| *H11m* | *AcclimSterC* Run3 | Model | 11 | 21187019 | 2.5E–08 | 14 | –4.20 | A | T | 174 | 15 | 22 | 7A | Loc_Os11g35980 [40], RAS suppressor; **Loc_Os11g36050 [0]**, chaperone PREFOLDIN; **Loc_Os11g36090 [26]**/Loc_Os11g36140 [58]/Loc_Os11g36150 [66]/Loc_Os11g36160 [76], serine/threonine kinase |
| *H1(1)m′* | *AcclimSterC* Run4 | Model | 1 | 11451409 | 2.5E–07 | 3 | –3.19 | A | T | 170 | 19 | 22 | 7B | **Loc_Os01g20160 [10]**, cation homeostasis, salinity; Loc_Os01g20206 [54], methyltransferase |
| *H1(2)m′* | *AcclimSterC* Run4 | Model | 1 | 39494385 | 1.0E–05 | 7 | –4.53 | C | T | 183 | 6 | 23 | 7B | **Loc_Os01g67890 [34]**, syn. *OsMADS96*, MADSbox TF; **Loc_Os01g67970 [2]**, syn. *JMJ705* (H3K27 histone demethylase) expressed in sperm cells and pollen; **Loc_Os01g67980 [8]**, leaf senescence; **Loc_Os01g68000 [31]**, orth.TEL1/ATM/PLA2, meiosis, plastochron, dwarfism; Loc_Os01g68020 [52], histone acetyl transferase |
| *H2(1)m′* | *AcclimSterC* Run4 | Model | 2 | 27031056 27051695 27164512 27394619 | 4.0E–06 | 38 | –3.48 | G | A | 178 | 11 | 17 | 7B | **Loc_Os02g44610 [1]**/**Loc_Os02g44642 [24]**/Loc_Os02g44920 [52]/**Loc_Os02g45130 [20]**/Loc_Os02g45170 [25], helix–loop–helix prot., MEKK serine/threonine kinase; **Loc_Os02g44630 [15]**, aquaporin, seed germination; Loc_Os02g44780 [41], geranylgeranyl-PP-synthase; **Loc_Os02g45110 [32]**, $N^6$-adenine RNA methyltransferase |
| *H2(2)m′* | *AcclimSterC* Run4 | Model | 2 | 34040198 | 5.0E–06 | 5 | –2.88 | C | A | 167 | 22 | 23 | 7B | **Loc_Os02g55560 [12]**, serine/threonine kinase; **Loc_Os02g55570 [8]**, meiotic chromosome segregation |
| *H6m′* | *AcclimSterC* Run4 | Model | 6 | 10122260 (locus 1) | 1.0E–10 | 11 | –6.80 | A | T | 182 | 7 | 22 | 7B | **Loc_Os06g17440 [0]**, microtubule assoc. prot.; **Loc_Os06g17490 [26]**, serine/threonine kinase; **Loc_Os06g17480 [16]**, OsHAP3D, histone-like TF expressed early in endosperm; Loc_Os06g17730 [59], plastocyanin, copper-binding |
| | | | | 10347284 (locus 2) | 1.0E–10 | 11 | –6.80 | A | T | 182 | 7 | 23 | 7B | **Loc_Os06g17840 [4]**, HEAT repeat prot., sister chromatid cohesion prot., meiosis; **Loc_Os06g17830 [5]**, Fe oxidoreductase; **Loc_Os06g17880 [31]**/Loc_Os06g17900[42]/Loc_Os06g17910 [51]/Loc_Os06g17920 [63]/Loc_Os06g17930 [77], apoptotic ATPases; blast resistance cluster |

**Table 3.** *Continued*

| QTL | Trait, model run | Variable type | Chr | Locus of smallest *P* (bp) | P | SNPs *P*<0.001 | Effect | Base pair | | Allele frequency (no. of cases) | | No. genes | Fig | Putative candidate genes: LOC_ annotation(MSU), (distance from SNP in kB), (common name and function using public databases) |
|---|---|---|---|---|---|---|---|---|---|---|---|---|---|---|
| *H7m′* | *AcclimSterC* Run4 | Model | 7 | 26293894 | 1.0E–05 | 13 | 5.02 | G | A | 182 | 7 | 26 | 7B | Loc_Os07g43870 [58], heat shock protein; **Loc_Os07g43950 [27]**, RNA binding nucl.acid splicing factor; **Loc_Os06g43980 [0]**, RNA helicase; **Loc_Os07g44040 [29]**, RAS family prot., submergence tol.; Loc_Os07g44090 [63], MYB-like TF |
| *H8m′* | *AcclimSterC* Run4 | Model | 8 | 5811180 | 2.0E–07 | 2 | –4.66 | G | T | 178 | 11 | 23 | 7B | **Loc_Os08g10070 [31]**/Loc_Os08g10150 [78], serine/threonine kinase; Loc_Os08g09940 [62], rRNA methyl transferase; Loc_Os08g09950 [58]/**Loc_Os08g10010 [23]**, FAD, fatty acid desaturase |
| *H9m′* | *AcclimSterC* Run4 | Model | 9 | 20203818 | 5.0E–07 | 17 | –4.34 | G | T | 178 | 11 | | 7B | Loc_Os09g34150 [44]/**Loc_Os09g34160 [29]**, apoptotic gene; **Loc_Os09g34214 [4]/Loc_Os09g34230 [11]/Loc_Os09g34250 [19]/Loc_Os09g34270 [27]**, UDP glucoronyl and glucosyl transf.; Loc_Os09g34320 [55], methyltransferase |
| *H11m′* | *AcclimSterC* Run4 | Model | 11 | 21187019 | 1.3E–09 | 17 | –4.57 | A | T | 174 | 15 | 22 | 7B | As in *H11m* |

(classified minor for low allelic frequency) and *Sc7m* (major; chr7, $P=4.0 \times 10^{-7}$, 9 supporting SNPs).

### *Genomic associations for cold acclimation*

*AcclimSterC*, when co-optimized with all model parameters participating in sterility simulation (Run3), yielded a single but strong association on chr11 (*H11m*; $P=2.5 \times 10^{-8}$) (Fig. 7A). Its allelic frequency was 8% and 14 SNPs supported it (Table 3). When the *KSterSlope* parameter was fixed (Run4, Fig. 7B), the significance of this QTL increased to $P=1.3 \times 10^{-9}$ (labelled *H11m′*), and eight new QTLs appeared on chr 1, 2, 6, 7, 8, and 9, with *P* between $1.0 \times 10^{-5}$ and $1.0 \times 10^{-10}$. The QTL *H2(1)m′* (chr2, $P=4.0 \times 10^{-6}$) occurred as four peaks separated by 21, 113 and 230 kb. Similarly, QTL *H6m′* (chr6, $P=1.0 \times 10^{-10}$) occurred as two peaks 225 kb apart. The corresponding genomic regions were not repetitive.

For acclimation QTLs we analysed the allelic subpopulations. Among all accessions carrying the positive-effect allele for *AcclimSterC*, 61% were traditional Madagascar varieties (which constituted 18% of the panel). In *H11m*/*H11m′*, 13 of 15 accessions (87%) having the acclimation allele were from Madagascar. In *H8m′* it was 91% and in *H1(2)m′*, 100%. Low proportions of Madagascar accessions having the acclimation allele occurred in *H1(1)m′* (21%) and *H9m′* (18%). Twelve Madagascar accessions had the positive allele ≥3 *AcclimSterC* QTLs. Non-Madagascar accessions carrying acclimation alleles on several QTLs were generally from India, notably cvs Gochi Boro, Kasalath, Bala and Badkalamkati.

### *Candidate genes*

In Table 3, putative candidate genes within ±100 kb and ±39 kb (±LD) of peak SNP are presented for the 18 major QTLs that had $P<1 \times 10^{-5}$, ≥3 supporting SNPs and allelic frequency ≥4% for the minor allele. Information on all 33 observed QTLs is presented in Supplementary Table S2. On average, 24 annotated genes were located within ±100kb of peak SNP, and nine within ±39 kb.

For QTLs for baseline sterility, functionally plausible candidate genes located closest to peak SNP were Loc_Os02g31140 in *Sb2(1)i*, involved in cuticle development; Loc_Os11g44170 in *Sb11i*, a calmodulin binding protein (with SNP located within the gene); Loc_Os06g47880 in *Sb6(2)m′* (colocalized with *Sb6(2)m*), a protein kinase controlling cell division; and Loc_Os08g43270 in *Sb8m′* (colocalized with *Sb8m*), an apoptotic gene involved in ROS stress protection. Several other genes of functional interest were located within LD, such as serine/threonine kinases. In *Sb8m*/*Sb8m′* a dehydration transcription factor (TF) (Loc_Os08g43200) and a heat shock protein involved in drought and salt tolerance (Loc_Os08g43334) were found. Genes of functional interest were also detected minor QTLs (see Supplementary Table S2).

For QTLs related to thermal stress, three major ones were found. For *Ss2i*, Loc_Os02g36924 is the *OsMADS27* flowering-related TF and Loc_Os02g36974 is a dynein protein.

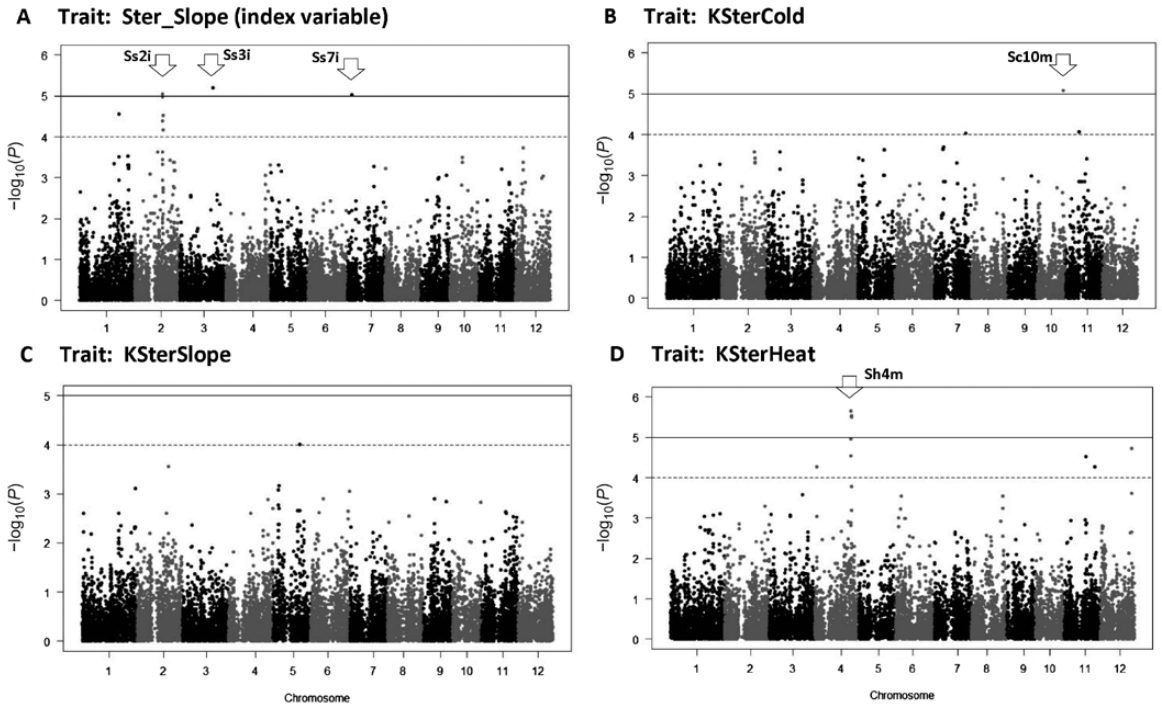


**Fig. 5.** Associations for spikelet sterility response to temperature. (A) Index variable *Ster_Slope*, derived from correlation of observed sterility *vs* $T_{min}$; (B) RIDEV parameter for critical temperature *KSterCold*; (C) RIDEV slope parameter *KSterSlope*; (D) RIDEV parameter for critical temperature *KSterHeat*. Results are for Estimation Run1 (Table 2).

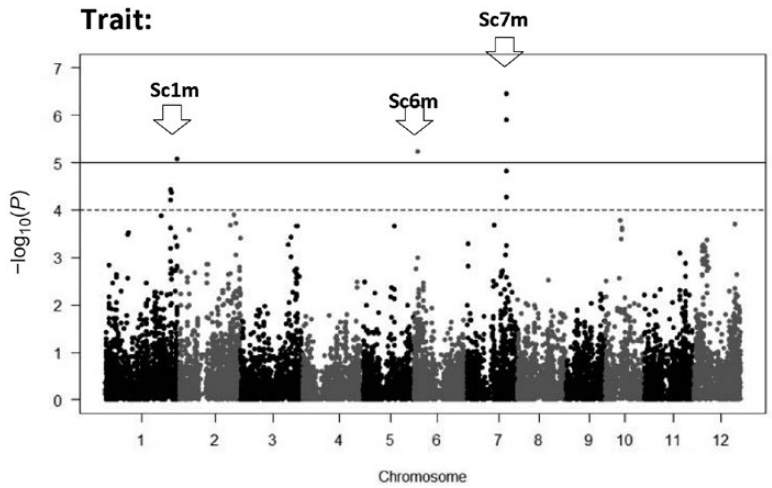


**Fig. 6.** GWAS associations for RIDEV parameter *KSterCold* as in Fig. 3B, but with *KSterSlope* fixed to constant value (Run2).

For *Sh4m*, five plausible functional candidates were observed, including a pollen protein, an H4 histone and a Zn-finger TF involved in growth regulation. For *Sc7m*, Loc_Os07g38730 was found near the peak SNP, a GTPase involved in reproductive development. Minor QTLs also had plausible candidate genes including RAS-family proteins, the important flowering gene *OsMADS56*, the squamosa-binding TF *OsSPL19* and a phytochrome-related gene involved in flowering control.

Eleven major QTLs were found for *AcclimSterC*. Several candidate genes potentially conveying epigenic expression control were associated with them, notably within ±20 kb a chaperone (*H11m*/*H11m´*, Loc_Os11g36050), a histone-like TF (*H6m´*, Loc_Os06g17480) and an RNA helicase (*H7m´*, Loc_Os06g43980). We also found serine/threonine kinases (*H2(1)m´*, Loc_Os02g55560; *H11m*, Loc_Os02g44610 and Loc_Os02g45130), a gene involved in meiosis (*H2(2)m´*, Loc_Os02g55570), and an androgen-induced sister chromatid cohesion factor (*H6m´*, Loc_Os06g17840). Within ±50 kb were an RNA methyltransferase (*H11m*, Loc_Os02g45110), an RNA-splicing MYB-like TF (*H7m´*, Loc_Os07g43950), a RAS protein (*H7m´*, Loc_Os07g44040) and a fatty acid desaturase (*H8m´*, Loc_Os08g10010). At 50–65 kb from the peak SNP, we found further putative epigenetic genes: a histone acetyltransferase (*H1(2)m´*, Loc_Os01g68020), two methyltransferases at (*H1(1)m´*, Loc_Os01g20206; *H9m´*, Loc_Os09g34320), and an rRNA methyltransferase (*H8m´*, Loc_Os08g09940).

In general, for direct thermal response of sterility, many genes functionally related to flowering, flower development or flower fertility were found. For cold acclimation, genes putatively conveying epigenetic control were frequent. Both types of gene functions were less frequent in QTLs for baseline sterility.

## Discussion

### *Heuristic estimation of thermal adaptation traits*

Physiological models have previously been used to extract environment response traits from phenotype data for genetic analyses (phenology: Nakagawa *et al.*, 2005; Yin *et al.*, 2005; morphogenic processes: Rebolledo *et al.*, 2015). Heuristic methods are useful when the raw phenotypic data contain underlying information that requires a physiological key to unlock. They are justified when the *a priori* physiological theory is sufficiently accurate.

The present study on sterility and its companion on phenology (Dingkuhn *et al.*, 2017) fitted RIDEV to 203 accessions across diverse climatic situations. The model explained 91% of variation of time to flowering, which increased further to 94% when cold acclimation was considered. For sterility, RIDEV explained only 38% of variation but this value nearly doubled to 64% when acclimation was considered. It thus seems that cold-stress hardening during earlier developmental phases is important for sterility responses in rice. The lower predictability of sterility as compared with phenology resided partly in error propagation (sterility prediction is sensitive to timing of stress-sensitive phases), but also in third causes of unfilled spikelets such as panicle architecture and assimilate supply (Sheoran and Sain, 1996).

RIDEV parameters gave mostly different but stronger QTLs as compared with the index variables that were more directly derived from observation. This raises the question of whether the parameters reflected precisely the physiological traits they were meant to express. Parameters were not functionally independent and thus absorbed some of each other's estimation errors (e.g. slope *vs* threshold parameters for thermal response). This problem is intrinsic to complex models and particularly to extracting different types of information (heat or cold sterility) from the variation of a single measured variable (unfilled spikelets), climate variation being the discriminating key. Good phenotype predictions thereby are no proof of biological accuracy.

Significant genomic associations with model parameters indicate that the model reflects a biological reality because measurements of phenotype and DNA polymorphisms are independent. The biological function of causative genes, once known, can further inform on the biological meaning of model parameters.

### *Control of unexplained baseline sterility*

Rice spikelet sterility is mostly male-derived and depends on pollen production, viability and load on the stigma (Saragih *et al.*, 2013). The developmental and genetic control of male sterility is well documented because of its importance for hybrid seed production (Wang *et al.*, 2013). Among many genes involved in the network, *OsMADS3* and *OsMADS58* are located upstream, controlling OsUDT1 (a helix–loop–helix protein) through OsMSP1 (a serine/threonine kinase). They control downstream pathways for pollen exine and tapetum development. Genes associated with meiosis were reported by Deveshwar *et al.* (2011), including *OsMSP1* and many cell-cycle controlling RAD genes.

These specific genes were not among our candidate genes. However, a protein kinase controlling the cell cycle, Loc_Os06g47880, was observed in major QTL *Sb6(2)m´* (<20 kb from SNP; $P$=4.0 × $10^{-8}$). It was located in close neighborhood to three serine/threonine kinases. We frequently encountered such clusters of functionally plausible candidate genes. Serine/threonine kinases, known for control functions in reproductive development and stress responses (Becraft, 2002), were also found near the center of three minor QTLs, in one case a cluster of four such genes (QTL *Sb2(2)m*). The main SNP of minor QTL *Sb1m´* was located within Loc_Os01g06590 (syn. *OsRHC4*), an anaphase controlling ringfinger gene. It is expressed in the panicle at pistil/stamen primordia differentiation stage IV, a pre-meiotic stage (Ma *et al.* 2009). Within 24 kb of this gene was a helix–loop–helix TF (Loc_Os01g06640) participating in anther development (Phytozome). At 39 kb from the SNP, an arginyl-tRNA synthase (Loc_Os01g06510) was located that is up-regulated in florets during meiosis under heat and cold stress, associated with male sterility (Pan *et al.*, 2014). This cluster of three genes in QTL *Sb1m´* linked to anther/microspore development and spikelet sterility, two of them during meiosis, is probably no coincidence. Mugford *et al.* (2013) reported operon-like, functional and physical gene clusters that are co-expressed and probably common in plants.

Apart from anther and pollen development, protection from oxidative stress is important for pollen viability because spikelets are exposed to desiccation, direct radiation and fluctuating temperatures. Major QTL *Sb8m* had the anti-apoptotic, ROS-protective, BCL2-type gene Loc_Os08g43270 at its center. This type of gene, when transformed in rice, was reported to induce tolerance to oxidative stress and salinity (Hoang *et al.*, 2015). Li *et al.* (2006) reported that apoptosis participates in tapetum development and male sterility.

Many candidate genes were involved in signaling. Two genes encoded ADB ribosylation factors (ARF GTPases: Loc_Os06g02390 in major QTL *Sb6(2)m*; Loc_Os02g42134 in minor QTL *Sb2(2)m*). Zhuang *et al.* (2005) reported that such genes exert developmental control through polar auxin transport in Arabidopsis. Du *et al.* (2011) confirmed developmental effects of ARF GTPases in rice via actin cytoskeletal organization and vesicle transport. Intracellular signaling frequently involves calcium via calmodulin. Wei *et al.* (2014) reported that a calcium-dependent protein kinase (OsCPK9) regulates spikelet fertility in rice. One such calmodulin-binding protein (Loc_Os11g44170) was the sole candidate gene for major QTL *Sb11i* (peak SNP located within the gene).

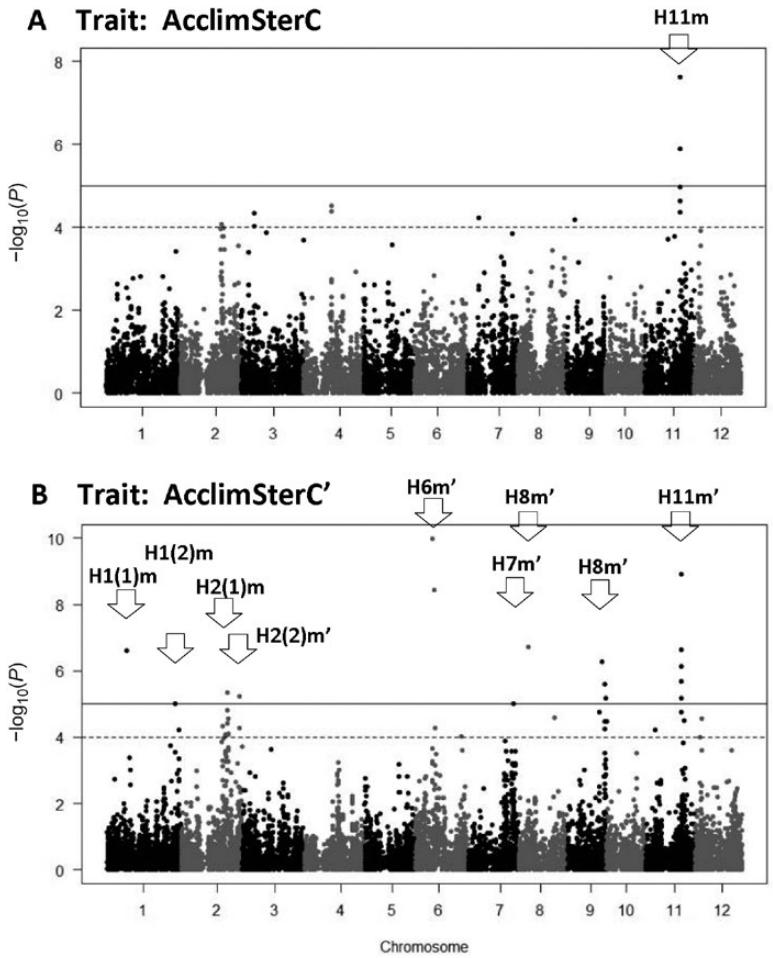


**Fig. 7.** Genomic associations for RIDEV *AcclimSterC* parameter. (A) Parameter estimation with *KSterSlope* co-fitted (Run3, Table 2); (B) Estimation with *KSterSlope* fixed (Run4).

The array of candidate genes for baseline sterility was diverse but this may be due to its multiple possible causes. In general, the abundance of plausible genes at the center of the QTLs supported their physiological function.

### *Baseline and thermal-sterility QTLs co-localize with MADS-box and other reproduction genes*

MADS-box and other reproduction genes were rare in QTLs for baseline sterility. *OsELF3* (syn. *HD17*, Loc_Os06g05060), exerting circadian control of flowering under long days (Yang *et al.*, 2013), was found in minor QTL *Sb6(1)i*. This gene, expressed in leaves during perception of the photoperiod stimulus, is also strongly expressed in anthers and pistils (http://rice.plantbiology.msu.edu/), and may thus be involved in spikelet fertility. Furthermore, Loc_Os01g06590 in *Sb1m´* (SNP located within gene) is an anaphase promoting Zn-finger TF. Its up-regulation under cold stresses (http://genevisible.com/) and expression in male gametes (http://genevisible.com/) makes this gene a causative candidate for spikelet fertility/sterility. *Sb1m´* was classified as a minor QTL because of low allelic frequency but had 19 supporting SNPs and $P=1.0 \times 10^{-5}$.

For thermal-stress-induced sterility, candidate genes *OsMADS56* (QTL *Sc10m*, classified as minor because it lacks supporting SNPs) and *OsMADS27* (minor QTL *Ss1i*) were found. *OsMADs96* was associated with *H1(2)m´*, a major QTL for cold acclimation. MADS-box genes are key to morphogenetic and flowering processes (Arora *et al.*, 2007). While *OsMADS56* is located upstream in the flowering network (Matsubara *et al.*, 2012; Shrestha *et al.*, 2014), *OsMADS27* has unknown function but is up-regulated under cold and salt stress (Arora *et al.*, 2007). *OsMADS96* is weakly but broadly expressed (albeit most strongly in pollen) and up-regulated under heat and drought (http://genevisible.com/).

Also related to flowering was Loc_Os01g72090 (QTL *Sc1m*, classified as minor due to low allelic frequency; 12 supporting SNPs; $P=7.9 \times 10^{-6}$), a ferredoxin oxidoreductase (phytochromobilin) involved in phytochrome biosynthesis and, putatively, photoperiodism (Phytozome). It shows protein–protein interaction (RiceNetDb) with the ELF3/HD17 found in QTL *Sb6(1)I* and is strongly expressed in the stigma (http://genevisible.com/). We furthermore found *OsSPL19* in minor QTL *Sh11m* (heat-sterility), a squamosa-binding TF putatively involved in floral development (Xie *et al.*, 2006). Its Arabidopsis homologue, *AtSPL13* (Zhu *et al.*, 2013), controls leaf appearance rate (Preston and Hileman, 2013) involving micro-RNA156 (Wang *et al.* 2008).

For cold acclimation QTLs we identified two meiosis-related candidate genes. Loc_Os01g68000, located close to

*OsMADS96* in major QTL *H1(2)m´*, is also called *PLA2* (*PLASTOCHRON2*) or *LHD2* (*LEAFYHEAD2*) and linked to floral development (http://pathway.iplantcollaborative.org). It encodes an MEI2-like protein, essential for meiosis in some species but unconfirmed for rice (Anderson *et al.*, 2004). The gene is expressed in pollen and down-regulated under drought, heat and cold (http://genevisible.com/). The other meiotic candidate gene was Loc_Os02g55570 (syn. *OsSGO1*; RICENCODE) in major QTL *H2(2)m´* associated with chromosome segregation (Phytozome) and centromer cohesion (OGRO).

These gene–QTL associations suggest linkages between genetic control of flowering and sterility.

### *RAS super-family genes and other GTPases are frequent in sterility QTLs*

The RAS super-family of small GTPases consists of five groups (Ras, Rho, Arf/Sar, Ran, and Rab). They are intracellular signaling nodes activated by extracellular stimuli, controlling gene expression for growth and differentiation (for review see Rojas *et al.*, 2012). Three RAS GTPases (Peng *et al.*, 2014; Xu and Cai, 2014) were associated with QTLs for thermal response of sterility. A RAS suppressor was found for major QTL *H11m* (cold acclimation), and ARF and RAB genes for baseline sterility QTLs. The Loc_Os01g53600 RAS-protein in minor QTL *Ss1i* is up-regulated under drought (http://genevisible.com/). An intriguing GTPase (Loc_Os07g38730) was found in major QTL *Sc7m*. It has a tubulin domain, is involved in flower development and leaf senescence, and is expressed during early inflorescence development (Expression Atlas, http://www.ebi.ac.uk/).

The role of these genes in spikelet sterility merits investigation. For example, Xu and Cai (2014) reported the involvement of *RAN1* in rice cold tolerance. Nielsen *et al.* (2008) reviewed the regulatory role of RAB and ARG GTPases in intracellular vesicle transport.

### *Serine/threonine kinases are omnipresent in sterility QTLs*

Many serine/threonine kinases link external signals to cellular development or defense responses, and are thus called stress proteins (Diédhiou *et al.*, 2008; Sinha *et al.*, 2011). For our 32 QTLs, 20 such kinases were genes found within 50 kb of the main SNP, and 36 within 100 kb, frequently in clusters. Most known abiotic-stress-related, receptor-like kinases respond to drought and few to cold (Gao and Xue, 2012). The regulatory function of most kinases is unknown due to their large number, however.

### *Candidate genes controlling physiological adaptation to abiotic stresses*

#### *Heat*

The strongest association for heat was major QTL *Sh4m*, with five interesting genes clustered within 20 kb of the main SNP. Peak SNP was located within Loc_Os04g49430, a Zn-finger TF regulating growth through OsPIN3 (an auxin transporter involved in drought response; Zhang *et al.*, 2012). Adjacent were an H4 histone, an RNA-binding protein, a MYB-type TF and a pollen lipoprotein, all potentially relevant. Loc_Os04g49430 combines an RCC1 domain involved in chromosome condensation and, thus, probably transcription control (http://www.ricechip.org/). It has a FYVE zinc finger domain known to be involved in lipid signaling (Wywial and Singh, 2010). Which parts of this gene cluster are involved in heat sterility merits investigation.

About 40 kb from *OsSPL19* on minor QTL *Sh11m* we found Loc_Os11g30410, a SUMO-type ubiquitation gene related to male sterility (ALOC_OS1/RAD31 component; Phytozome). Reversible protein ubiquitation is important for heat stress adaptation (Miller and Vierstra, 2011).

#### *Cold stress*

Proline accumulation is a stress defense involved in cold tolerance, osmoregulation and maintenance of cytoplasmic integrity (Hayat *et al.*, 2012). A proline synthase co-expressed protein (expressed under drought; PlaNet) was found in minor QTL *Sc1m* and a prolyl-tRNA synthase in QTL *Ss7i* (minor due to few supporting SNPs) (http://ricexpro.dna.affrc.go.jp/). More candidate genes were related to oxidative stress, most frequently in baseline-sterility QTLs (*Sb6(1)i* and *Sb6(1)m*, minor; *Sb6(2)m*, major). Cold-sterility QTL *Sc1m´* (classified as minor due to low allelic frequency) had a cluster of six glutathione transferases (GST) at its center, with one (Loc_Os01g72130) strongly expressed in anthers and ovary (http://ricexpro.dna.affrc.go.jp/). Pereira da Cruz *et al.* (2013) reported that rice GST genes are up-regulated under cold stress and help in controlling oxidative stress. Loc_Os01g72130 is thus a promising candidate for cold tolerance.

A candidate gene for baseline sterility (major QTL *Sb2(1)i*) but potentially acting through desiccation avoidance was Loc_Os02g31140, a curly-leaf factor controlling cuticle development (OGRO) strongly expressed during early florescence development (http://ricexpro.dna.affrc.go.jp/). Anther cuticle development is important for spikelet fertility (Li and Zhang, 2010). Specifically expressed during early anther development (http://ricexpro.dna.affrc.go.jp/) is also Loc_Os01g06640, a helix–loop–helix (HLH) TF detected in major QTL *Sb6(2)m´* ($P$=4.0 × $10^{-8}$). The *bHLH* gene family is associated with control of cell/organ size and development (Heang and Sassa, 2012) and stress responses (Lima *et al.*, 2015). Fu *et al.* (2014) reported a *bHLH* gene acting as central switch in anther development.

An interesting gene at the center of QTL *Ss7i* (classified as minor due to few supporting SNPs) was O207g07170, a plastocyanin-domain gene expressed in pollen and flag leaves (http://genevisible.com/), and up-regulated under cold stress. Its two orthologs in *Citrus clementina* were identified as plantacyanins (Phytozome). Plantacyanins control directional pollen tube growth in Arabidopsis (Dong *et al.*, 2005).

#### *Cold acclimation and epigenetics*

Shimono *et al.* (2010) reported cold acclimation of spikelets pre-induced by stress during the vegetative stage. Adaptations

triggered by previously experienced conditions are likely caused by epigenetic control of gene expression. They are restricted to the organism's life cycle or carried into subsequent generations. Major mechanisms are histone methylation or acetylation and DNA methylation (Chinnusamy and Zhu, 2009), or on a post-transcriptional basis RNA modifications (Balint *et al.*, 2005). Hu *et al.* (2015) recently reported rice DNA methylomes related to environment-induced male sterility.

The cold-acclimation QTLs were rich in putative epigenetic genes, e.g. a histone-like TF (OsHAP3D in QTL *H6m´*, $P$=1.0 × $10^{-10}$), a histone acetyltransferase (*H1(2)m´*), an adenine RNA methyltransferase (*H2(1)m´*), an rRNA methyltransferase (*H8m´*), three unspecified methyltransferases, an RNA helicase (*H7m´*) and chaperones. The H3K27 histone demethylase Loc_Os01g67970 (syn. *JMJ705*) in QTL *H1(2)m´* was described by Li *et al.* (2013) and Shi *et al.* (2015) as being involved in epigenetic control of flowering. It is predominantly expressed in rice sperm cells and pollen (http://genevisible.com/).

Although the acclimation QTLs stood out for the abundance of putative epigenetics genes, a variety of other candidate genes were also identified. Loc_Os08g10010 in QTL *H8m´* encodes a fatty acid desaturase (FAD) highly expressed in the stigma (http://genevisible.com/). Cold-tolerant rices increase membrane fluidity through fatty acid desaturation when chilled (Pereira da Cruz *et al.*, 2009). Nair *et al.* (2009) demonstrated that expression of *OsFAD8* in rice is necessary to express cold tolerance.

Epigenetic control of responses to thermal stresses in plants is poorly understood. Its experimental study requires stress treatments at various developmental stages. Our results suggest that epigenetic control of cold adaptation is important in rice, particularly where chilling occurs early enough for acclimation. This is the case in the Madagascar highlands, and indeed we observed acclimation alleles predominantly in traditional rices from there. Radanielina *et al.* (2013) and Dingkuhn *et al.* (2015*a*) reported this group to be cold tolerant and genetically distinct.

### *Functional intersection between phenology and spikelet sterility*

The companion paper on phenology and this study on spikelet sterility will enable the construction of physiological and genetic control networks but this is beyond this paper's scope. It appears that phenology not only affects sterility through the timing of stress exposure (Dingkuhn, 1995). The control of both flowering and spikelet fertility depends on networks controlling development processes, involving some gene families best known to control flowering (e.g. *OsMADS*). This is unlikely to be an artifact of incomplete separation between traits by RIDEV because sterility and flowering date were independent measurements and the model accounted for phenology when relating sterility to temperature.

### *Perspectives*

It is hoped that this research will enhance breeding for adaptation to adverse and variable climates. The present and the companion study defined physiological component traits through crop-model assisted dissection of phenomics data. They produced QTLs and candidate genes on 203 accessions. The next steps are to narrow down the candidate genes by haplotype analysis using a new 700 000-SNP array (McCouch *et al.*, 2016) and re-sequenced genomes, and to construct integrated gene networks. For causative SNPs, once discovered, a promising shortcut to crop improvement will be CRISPR/Cas9-based genome editing (Bortesi and Fischer, 2015) to express them in elite backgrounds, both for validation and developing climate-change resilient varieties.

## Supplementary data

Supplementary data are available at *JXB* online.

Protocol S1. C++ code for RIDEV.

Fig. S1. Genetic structure of panel.

Fig. S2. Quantile–quantile (QQ) plots for Manhattan plots.

Fig. S3. Diurnal template for temperature dynamics used for hourly calculations.

Fig. S4. Frequency distributions of index variables.

Fig. S5. Sensitivity analysis of RIDEV simulations to variation of crop parameters.

Table S1. List of germplasm.

Table S2. Complete lists of GWAS associations.

Table S3. RIDEV V2 parameters and input/output variables.

## Acknowledgements

The authors would like to thank Drs Brigitte Courtois and Nourollah Ahmadi for valuable assistance in data analysis, as well as the excellent field staff of Africa Rice Center in Senegal and the Cirad-FOFIFA team in Madagascar.

## References

**Anderson GH, Alvarez ND, Gilman C, Jeffares DC, Trainor VC, Hanson MR, Veit B.** 2004. Diversification of genes encoding mei2-like RNA binding proteins in plants. Plant Molecular Biology **54,** 653–670.

**Arora R, Agarwal P, Ray S, Singh AK, Singh VP, Tyagi AK, Kapoor S.** 2007. MADS-box gene family in rice: genome-wide identification, organization and expression profiling during reproductive development and stress. BMC Genomics **8,** 242.

**Balint BL, Szanto A, Madi A, Bauer UM, Gabor P, Benko S, Puskás LG, Davies PJ, Nagy L.** 2005. Arginine methylation provides epigenetic transcription memory for retinoid-induced differentiation in myeloid cells. Molecular and Cellular Biology **25,** 5648–5663.

**Becraft PW.** 2002. Receptor kinase signaling in plant development. Annual Review of Cell and Developmental Biology **18,** 163–192.

**Bortesi L, Fischer R.** 2015. The CRISPR/Cas9 system for plant genome editing and beyond. Biotechnology Advances **33,** 41–52.

**Bradbury PJ, Zhang Z, Kroon DE, Casstevens TM, Ramdoss Y, Buckler ES.** 2007. TASSEL: software for association mapping of complex traits in diverse samples. Bioinformatics **23,** 2633–2635.

**Chinnusamy V, Zhu JK.** 2009. Epigenetic regulation of stress responses in plants. Current Opinion in Plant Biology **12,** 133–139.

**Courtois B, Audebert A, Dardou A, *et al.*** 2013. Genome-wide association mapping of root traits in a japonica rice panel. PLoS ONE **8,** e78037.

**De Storme N, Geelen D.** 2014. The impact of environmental stress on male reproductive development in plants: biological processes and molecular mechanisms. Plant, Cell & Environment **37,** 1–18.

**Deveshwar P, Bovill WD, Sharma R, Able JA, Kapoor S.** 2011. Analysis of anther transcriptomes to identify genes contributing to meiosis and male gametophyte development in rice. BMC Plant Biology **11,** 78.

**Diédhiou CJ, Popova OV, Dietz KJ, Golldack D.** 2008. The SNF1-type serine-threonine protein kinase *SAPK4* regulates stress-responsive gene expression in rice. BMC Plant Biology **8,** 49.

**Dingkuhn M, Sow A, Samb A, Diack S, Asch F.** 1995. Climatic determinants of irrigated rice performance in the Sahel. I. Photothermal and microclimatic responses of flowering. Agricultural Systems **48,** 385–410.

**Dingkuhn M, Miezan KM.** 1995. Climatic determinants of irrigated rice performance in the Sahel. II. Validation of photothermal constants and characterization of genotypes. Agricultural Systems **48,** 411–434.

**Dingkuhn M.** 1995. Climatic determinants of irrigated rice performance in the Sahel. III. Characterizing environments by simulating the crop's photothermal responses. Agricultural Systems **48,** 435–456.

**Dingkuhn M, Kouressy M, Vaksmann M, Clerget B, Chantereau J.** 2008. Applying to sorghum photoperiodism the concept of threshold-lowering during prolonged appetence. European Journal of Agronomy **28,** 74–89.

**Dingkuhn M, Pasco R, Pasuquin J, *et al*.** 2017. Crop-model assisted phenomics and genome-wide association study for climate adaptation of *indica* rice. 1. Phenology. Journal of Experimental Botany.

**Dingkuhn M, Radanielina T, Raboin L-M, *et al*.** 2015*a*. Field phenomics for response of a rice diversity panel to ten environments in Senegal and Madagascar. 2. Chilling-induced spikelet sterility. Field Crops Research **183,** 282–293.

**Dingkuhn M, Sow A, Manneh B, *et al*.** 2015*b*. Field phenomics for response of a rice diversity panel to ten environments in Senegal and Madagascar. 1. Plant phenological traits. Field Crops Research **183,** 342–355.

**Dong J, Kim ST, Lord EM.** 2005. Plantacyanin plays a role in reproduction in Arabidopsis. Plant Physiology **138,** 778–789.

**Du C, Xu Y, Wang Y, Chong K.** 2011. Adenosine diphosphate ribosylation factor-GTPase-activating protein stimulates the transport of AUX1 endosome, which relies on actin cytoskeletal organization in rice root development. Journal of Integrative Plant Biology **53,** 698–709.

**Fu Z, Yu J, Cheng X, Zong X, Xu J, Chen M, Li Z, Zhang D, Liang W.** 2014. The rice basic helix-loop-helix transcription factor TDR INTERACTING PROTEIN2 is a central switch in early anther development. The Plant Cell **26,** 1512–1524.

**Fu G-F, Zhang C-X, Yang Y-J, Xiong J, Yang X-Q, Zhang X-F, Jin Q-Y, Tao L-X.** 2015. Male parent plays a more important role in heat tolerance in three-line hybrid rice. Rice Science **22,** 116–122.

**Gao LL, Xue HW.** 2012. Global analysis of expression profiles of rice receptor-like kinase genes. Molecular Plant **5,** 143–153.

**Garavito A, Guyot R, Lozano J, Gavory F, Samain S, Panaud O, Tohme J, Ghesquière A, Lorieux M.** 2010. A genetic model for the female sterility barrier between Asian and African cultivated rice species. Genetics **185,** 1425–1440.

**Hayat S, Hayat Q, Alyemeni MN, Wani AS, Pichtel J, Ahmad A.** 2012. Role of proline under changing environments: a review. Plant Signaling & Behavior **7,** 1456–1466.

**Heang D, Sassa H.** 2012. Antagonistic actions of HLH/bHLH proteins are involved in grain length and weight in rice. PLoS ONE **7,** e31325.

**Hoang TM, Moghaddam L, Williams B, Khanna H, Dale J, Mundree SG.** 2015. Development of salinity tolerance in rice by constitutive-overexpression of genes involved in the regulation of programmed cell death. Frontiers in Plant Science **6,** 175.

**Hu J, Chen X, Zhang H, Ding Y.** 2015. Genome-wide analysis of DNA methylation in photoperiod- and thermo-sensitive male sterile rice Peiai 64S. BMC Genomics **16,** 102.

**Jagadish SV, Craufurd PQ, Wheeler TR.** 2007. High temperature stress and spikelet fertility in rice (*Oryza sativa* L.). Journal of Experimental Botany **58,** 1627–1635.

**Julia C, Dingkuhn M.** 2012. Variation in time of day of anthesis in rice in different climatic environments. European Journal of Agronomy **43,** 166–174.

**Julia C, Dingkuhn M.** 2013. Predicting heat induced sterility of rice spikelets requires simulation of crop-generated microclimate. European Journal of Agronomy **49,** 50–60.

**Li H, Zhang D.** 2010. Biosynthesis of anther cuticle and pollen exine in rice. Plant Signaling & Behavior **5,** 1121–1123.

**Li N, Zhang DS, Liu HS, *et al*.** 2006. The rice tapetum degeneration retardation gene is required for tapetum degradation and anther development. The Plant Cell **18,** 2999–3014.

**Li T, Chen X, Zhong X, *et al*.** 2013. Jumonji C domain protein JMJ705-mediated removal of histone H3 lysine 27 trimethylation is involved in defense-related gene activation in rice. The Plant Cell **25,** 4725–4736.

**Lima JM, Nath M, Dokku P, *et al*.** 2015. Physiological, anatomical and transcriptional alterations in a rice mutant leading to enhanced water stress tolerance. AoB Plants **7,** plv023.

**Long Y, Zhao L, Niu B, *et al*.** 2008. Hybrid male sterility in rice controlled by interaction between divergent alleles of two adjacent genes. Proceedings of the National Academy of Sciences, USA **105,** 18871–18876.

**Ma K, Xiao J, Li X, Zhang Q, Lian X.** 2009. Sequence and expression analysis of the C3HC4-type RING finger gene family in rice. Gene **444,** 33–45.

**Matsubara K, Ogiso-Tanaka E, Hori K, Ebana K, Ando T, Yano M.** 2012. Natural variation in *Hd17*, a homolog of *Arabidopsis ELF3* that is involved in rice photoperiodic flowering. Plant & Cell Physiology **53,** 709–716.

**McCouch SR, Wright MH, Tung CW, *et al*.** 2016. Open access resources for genome-wide association mapping in rice. Nature Communications **7,** 10532.

**Miller MJ, Vierstra RD.** 2011. Mass spectrometric identification of SUMO substrates provides insights into heat stress-induced SUMOylation in plants. Plant Signaling & Behavior **6,** 130–133.

**Mugford ST, Louvean T, Melton R, *et al*.** 2013. Modularity of plant metabolic gene clusters: A trio of linked genes that are collectively required for acylation of triterpenes in oat. The Plant Cell **25,** 1078–1092.

**Nakagawa H, Yamagishi J, Miyamoto N, Motoyama M, Yano M, Nemoto K.** 2005. Flowering response of rice to photoperiod and temperature: a QTL analysis using a phenological model. Theoretical and Applied Genetics **110,** 778–786.

**Nair PMG, Kang IN, Moon B-Y, Lee C-H.** 2009. Effects of low temperature stress on rice (*Oryza sativa* L.) plastid ω-3 desaturase gene, *OsFAD8* and its functional analysis using T-DNA mutants. Plant Cell Tissue and Organ Culture **98,** 87–96.

**Nielsen E, Cheung AY, Ueda T.** 2008. The regulatory RAB and ARF GTPases for vesicular trafficking. Plant Physiology **147,** 1516–1526.

**O'Toole JC, Namuco OS.** 1983. Role of panicle exertion in water stress induced sterility. Crop Science **23,** 1093–1097.

**Pan Y, Li Q, Wang Z, Wang Y, Ma R, Zhu L, He G, Chen R.** 2014. Genes associated with thermosensitive genic male sterility in rice identified by comparative expression profiling. BMC Genomics **15,** 1114.

**Peng X, Ding X, Chang T, Wang Z, Liu R, Zeng X, Cai Y, Zhu Y.** 2014. Overexpression of a vesicle trafficking gene, OsRab7, enhances salt tolerance in rice. The Scientific World Journal **2014,** 483526.

**Pereira da Cruz R, Ineu Golombieski J, Taís Bazana M, Cabreira C, Foletto Silveira T, Picolli da Silva L.** 2009. Alterations in fatty acid composition due to cold exposure at the vegetative stage in rice. Brazilian Journal of Plant Physiology **22,** 199–207.

**Pereira da Cruz PA, Cargnelutti D, Adamski JM, de Reitas Terra T, Fett JP.** 2013. Avoiding damage and achieving cold tolerance in rice plants. Food and Energy Security **2,** 96–119.

**Preston JC, Hileman LC.** 2013. Functional evolution in the plant *SQUAMOSA-PROMOTER BINDING PROTEIN-LIKE* (*SPL*) gene family. Frontiers in Plant Science **4,** 80.

**Radanielina T, Ramanantsoanirina A, Raboin L-M, Frouin J, Perrier X, Brabant P, Ahmadi N.** 2013. The original features of rice (*Oryza sativa* L.) genetic diversity and the importance of within-variety diversity in the highlands of Madagascar build a strong case for in situ conservation. Genetic Resources and Crop Evolution **60,** 311–323.

**Rebolledo MC, Dingkuhn M, Courtois B, Gibon Y, Clément-Vidal A, Cruz DF, Duitama J, Lorieux M, Luquet D.** 2015. Phenotypic and genetic dissection of component traits for early vigour in rice using plant growth modelling, sugar content analyses and association mapping. Journal of Experimental Botany **66,** 5555–5566.

**Reymond M, Muller B, Leonardi A, Charcosset A, Tardieu F.** 2003. Combining quantitative trait loci analysis and an ecophysiological model to analyze the genetic variability of the responses of maize leaf growth to temperature and water deficit. Plant Physiology **131,** 664–675.

**Rojas AM, Fuentes G, Rausell A, Valencia A.** 2012. The Ras protein superfamily: evolutionary tree and role of conserved amino acids. The Journal of Cell Biology **196,** 189–201.

**Saragih AA, Pteh AB, Ismail MR, Mondal MMA.** 2013. Pollen quality traits of cultivated (*Oryza sativa* L. ssp. indica) and weedy (*Oryza sativa* var. nivara) rice to water stress at reproductive stage. Australian Journal of Crop Science **7,** 1106–1112.

**Sheoran IS, Sain HS.** 1996. Drought-induced male sterility in rice: Changes in carbohydrate levels and enzyme activities associated with the inhibition of starch accumulation in pollen. Sexual Plant Reproduction **9,** 161–169.

**Shi J, Dong A, Shen W-H.** 2015. Epigenetic regulation of rice flowering and reproduction. Frontiers in Plant Science **5,** 803.

**Shimono H, Ishii A, Kanda E, Suto M, Nagano K.** 2010. Genotypic variation in rice cold tolerance responses during reproductive growth as a function of water temperature during vegetative growth. Crop Science **51,** 290–297.

**Shrestha R, Gómez-Ariza J, Brambilla V, Fornara F.** 2014. Molecular control of seasonal flowering in rice, arabidopsis and temperate cereals. Annals of Botany **114,** 1445–1458.

**Sinha AK, Jaggi M, Raghuram B, Tuteja N.** 2011. Mitogen-activated protein kinase signaling in plants under abiotic stress. Plant Signaling & Behavior **6,** 196–203.

**Sved JA.** 1971. Linkage disequilibrium and homozygosity of chromosome segments in finite populations. Theoretical Population Biology **2,** 125–241.

**Wang JW, Schwab R, Czech B, Mica E, Weigel D.** 2008. Dual effects of miR156-targeted *SPL* genes and *CYP78A5/KLUH* on plastochron length and organ size in *Arabidopsis thaliana*. The Plant Cell **20,** 1231–1243.

**Wang K, Peng X, Ji Y, Zhu Y, Li S.** 2013. Gene, protein and network of male sterility in rice. Frontiers in Plant Science **4,** 92.

**Wei S, Hu W, Deng X, *et al*.** 2014. A rice calcium-dependent protein kinase OsCPK9 positively regulates drought stress tolerance and spikelet fertility. BMC Plant Biology **14,** 133.

**Wolters-Arts M, Mariani C, Rieu I.** 2013. Ensuring reproduction at high temperatures: The heat stress response during anther and pollen development. Plants **2,** 489–506.

**Wopereis MCS, Haefele SM, Dingkuhn M, Sow A.** 2003. Decision support tools for irrgated rice-based systems in the Sahel. In: Struif Bontkes TE, Wopereis MCS, eds. A practical guide to decision-support tools for agricultural productivity and soil fertility enhancement in sub-Saharan Africa. Wageningen, The Netherlands: IFDC and CTA, 114–126.

**Wywial E, Singh SM.** 2010. Identification and structural characterization of FYVE domain-containing proteins of *Arabidopsis thaliana*. BMC Plant Biology **10,** 157.

**Xie K, Wu C, Xiong L.** 2006. Genomic organization, differential expression, and interaction of SQUAMOSA promoter-binding-like transcription factors and microRNA156 in rice. Plant Physiology **142,** 280–293.

**Xu P, Cai W.** 2014. *RAN1* is involved in plant cold resistance and development in rice (*Oryza sativa*). Journal of Experimental Botany **65,** 3277–3287.

**Yang J, Zhang J.** 2010. Grain-filling problem in 'super' rice. Journal of Experimental Botany **61,** 1–5.

**Yang Y, Peng Q, Chen GX, Li XH, Wu CY.** 2013. OsELF3 is involved in circadian clock regulation for promoting flowering under long-day conditions in rice. Molecular Plant **6,** 202–215.

**Yin X, Struik PC, van Eeuwijk FA, Stam P, Tang J.** 2005. QTL analysis and QTL-based prediction of flowering phenology in recombinant inbred lines of barley. Journal of Experimental Botany **56,** 967–976.

**Zhang Q, Li J, Zhang W, *et al*.** 2012. The putative auxin efflux carrier OsPIN3t is involved in the drought stress response and drought tolerance. The Plant Journal **72,** 805–816.

**Zhu Z, Tan L, Fu Y, *et al*.** 2013. Genetic control of inflorescence architecture during rice domestication. Nature Communications **4,** 2200.

**Zhuang X, Xu Y, Chong K, Lan L, Xue Y, Xu Z.** 2005. OsAGAP, an ARF-GAP from rice, regulates root development mediated by auxin in Arabidopsis. Plant, Cell & Environment **28,** 147–156.